

CHAPTER IV

DESIGNING MICROSTRUCTURE OF NANOPOROUS CARBON AS A CATALYST SUPPORT FOR BIODIESEL PRODUCTION

4.1 Abstract

Nanoporous carbon materials prepared from polybenzoxazine precursor have been used as catalyst supports for biodiesel upgrading. In this study, polybenzoxazine was synthesized from 1,6-hexamethylene diamine, bisphenol-A, and formaldehyde while silica particles were used as templates to attain controllable mesoporous carbons. SEM micrographs revealed that the obtained carbons consisted of interconnected 3D particles. The BET confirmed 327 m²/g surface area, 3.741 cc/g pore volume, and 24.2 nm average pore size. For biodiesel upgrading, the conversion of methyl linoleate (C 18:2) to methyl oleate (C 18:1) for partial hydrogenation by using Pd(NH₃)₄Cl₂ supported on carbon materials (Pd/porous carbon) was investigated. The effect of the carbon microstructure on the upgrading performance was compared with commercial microporous activated carbon. Palladium (Pd) mesoporous supports exhibited higher catalytic activity than microporous catalyst in the hydrogenation reaction.

Keywords : Nanoporous carbon/ Catalyst support/ Biodiesel/ Partial hydrogenation

4.2 Introduction

Biodiesel or fatty acid methyl ester (FAME) is known to be a good alternative choice to replace petroleum-based diesel. The advantages of biodiesel are: renewability, biodegradability, higher flash point, higher cetane number, reduction of exhaust emissions, miscibility with petroleum-based diesel, and its ability to be produced domestically. Biodiesel produced from vegetable oil that contains higher unsaturated fatty acid composition exhibits lower oxidative stability. In contrast, the higher the saturated fatty acid composition, the worse cold flow properties become. Therefore, the partial hydrogenation of polyunsaturated FAMEs to monounsaturated

ones is a promising solution to these problems. Moreover, noble metals such as Pd seem to be the most promising catalyst. Supported Pd catalysts have been widely used as catalysts for the hydrogenation reaction. The materials usually used as a catalyst support are: carbon, silica, alumina, and zeolite. Due to the difference in nature and structure of each support, the type of support is believed to effect on the catalytic activity and selectivity of the catalyst. Moreover, the same support with different pore sizes also effects on the rate and selectivity of the reaction.

Since the 1990s, resorcinol-formaldehyde organic gels have received considerable attention as porous carbon precursors due to their unique properties, such as high surface areas and controlled porous structures. Starting from the first report by Pekala (Pekala *et al.*, 1989), research has been focused on achieving and controlling the degree of meso/macroporosity of these carbon materials and on modifying the synthesis procedures. From the reaction engineering point of view, when working either in the liquid- or gas-phase, the use of non-microporous materials is considered highly desirable in order to avoid internal mass-transfer limitations. Three different types of carbon gels can be obtained depending on the solvent drying method : aerogels (drying under supercritical CO₂), xerogels (drying at ambient temperature and pressure conditions) and cryogels (freeze drying). Depending on the pH and the dilution ratio of the starting resorcinol formaldehyde precursor solution, these materials can present widely different textures. Carbon xerogels have been used as catalyst supports in fuel cells, using metals like Pt, Pd, and Ru in fine chemical applications. Polybenzoxazine (PBZ) provides high thermal stability, good flame retardant, low shrinkage upon polymerization, no by-products or volatile generation, excellent dimensional stability, and rich molecular design flexibility. In addition, the supercritical drying process is not necessary due to high crosslink density of polybenzoxazine (Ishida *et al.*, 1996).

In this study, carbon xerogels derived from polybenzoxazine with BET surface area of 327 m²/g and pore size of 25 nm were produced by modifying a previously described ambient-pressure drying method and then used as a Pd catalyst support for the partial hydrogenation process. The carbon xerogel supported Pd, abbreviated as Pd/Cx, were characterized by electron microscopy techniques (SEM,

TEM). The catalytic activity of these samples were also investigated in comparison with those of Pd catalyst on activated carbon and silica dioxide (SiO_2)

4.3 Experiment

4.3.1 Polybenzoxazine Preparation

Bisphenol-A was dissolved in dioxane and magnetically stirred for 20 min before mixed with formaldehyde, silica colloids, CTAB (cetyltrimethylammonium bromide) and hexamethylenediamine (HAD), respectively. The mixture was then continuously stirred for 1 h before putting in a closed system and heating at 80°C for 2 days in an oil bath to let the gel set. After that, CTAB and solvent were removed by ambient pressure drying. The resulting organogel was cured at 160°C and 180°C for 3 h at each temperature, and 200°C for 1 h to obtain the fully-cured polybenzoxazine.

4.3.2 Pyrolysis Process

Fully-cured polybenzoxazine xerogels were pyrolyzed under nitrogen flow at 800°C , followed by cooling to room temperature. Finally, silica colloids were removed from carbon xerogels (CX) by immersing in hydrofluoric acid for 24 h.

4.3.3 Catalyst Preparation

Commercial activated carbon (AC) with an average pore diameter of 3.6 nm, carbon xerogels (CX) with an average pore diameter of 25 nm and commercial silica (SiO_2) with an average pore diameter of 30 nm were used as supports to study the effect of pore size on the catalytic activity. The sample was prepared by incipient wetness impregnation with an aqueous solution containing appropriate amounts of $\text{Pd}(\text{NH}_3)_4\cdot\text{Cl}_2$. The total amount of Pd loading was 1 wt%. After impregnation, the catalyst was dried by a rotary evaporator and calcined at 300°C under nitrogen flow. In case of SiO_2 , it was reduced under hydrogen stream at 300°C before the catalytic activity test. The prepared Pd supported on AC, CX and SiO_2 catalysts are abbreviated as Pd/AC, Pd/CX and Pd/ SiO_2 respectively.

4.3.4 Tranesterification of Soybean Oil

Fatty acid methyl esters (FAMES) of soybean oil were prepared by a typical transesterification reaction catalyzed by potassium hydroxide (KOH). The reaction took place in a three-necked round-bottomed flask. The amount of catalyst used was 1 wt.% compared to the starting rapeseed oil with 9:1 methanol to oil molar ratio. KOH was dissolved in methanol and added into the oil. The mixture was stirred at 60 °C for 2 h and cooled down. A phase separation was followed; the lower glycerine phase was removed. The upper phase was washed with 60 °C distilled water several times to remove remaining KOH, methanol, and possible soap. Finally, soybean biodiesel fuel (SBD) was dried by using sodium sulphate (Na_2SO_4) to remove the remaining washed water.

4.3.5 Partial Hydrogenation of FAMES

The partial hydrogenation reaction was carried out in a stainless steel semi-batch reactor at a temperature and hydrogen partial pressure of 120 °C and 4 bar, respectively. The stirring rate was maintained at 1000 rpm and the flow rate of hydrogen gas was 150 ml/min. The reactor was charged with approximately 180 ml of SDF feed and 1 wt% of Pd/AC, Pd/CX and Pd/SiO₂ catalyst. The reactor was connected to the reaction line and the system was purged with nitrogen. The reaction proceeded under the desired conditions. Finally, the liquid products were collected every 30 min. The total reaction time was 4 h.

4.3.6 Biodiesel Analysis

4.3.6.1 Gas Chromatography (GC)

Biodiesel and partial hydrogenated biodiesel will be identified the composition of C12:0, C14:0, C16:0, C18:0, C18:1, C18:2 and C22:0 by Hewlett Packard gas chromatograph 5890 Series II. The GC equipped with a flame ionization detector (FID) and a DB-WAX (30 m x 0.25 mm) fused-silica capillary column coated with a 0.1 µm film will be used. A carrier gas will be helium (99.99%) with a flow rate of 70 ml/min. The fatty acids will be quantified by injecting 0.2 µl of each sample. The injector and detector temperatures will be set at 200 °C with a split ratio

of 75:1 and 230 °C, respectively. The oven temperature will be initially at 130 °C after an isothermal period of 2 min, then increased to 220 °C with a rate of 2 °C/min and held for 15 min with the total analysis time of 62 min. FAME composition will be identified from the fraction of the area under the peak at different retention times.

4.3.6.2 Rancimat Testing

Oxidative stability is an important criterion for evaluating biodiesel quality. Because of its content of polyunsaturated methyl esters (FAME), which have several double bonds and oxidize easily so it effects on vehicle system. Oxidative stability will be analyzed according to European standard UNE-EN 14212:2003 method using a Metrohm 743 Rancimat instrument (Herisau, Switzerland). Sample of 3 g will be analyzed at a heating block temperature of 110 °C with the temperature correction factor (ΔT) of 0.98 °C, and a constant air flow of 10 L/h. The volatile compounds formed will be collected in the conductivity cell of 50 ml of DI water. The inflection point of the derivative curve of conductivity as a function of time will be reported as the induction period (IP, h). All the measurements will be performed in duplicate (Wadumesthrige et al., 2009).

4.3.6.3 Cold Flow Properties Testing

Two of major problems associated with the use of biodiesel are its oxidation stability and its cold flow properties, which can be indicated by cloud points (CP) and pour points (PP), which are important indices related to low-temperature operability of diesel fuels.

Pour Point

Pour point is the temperature at which a fuel can no longer be poured due to gel formation, while the cold filter plugging point is the temperature at which a fuel jams the filter due to the formation of agglomerates of crystals. The pour point measurement will be done as ASTM D97-D96a, biodiesel sample will be cooled inside a cooling bath to allow the formation of paraffin wax crystals. At about 9 °C above the expected pour point, and for every subsequent 3 °C, the test jar will be removed and tilted to check for surface movement. When the biodiesel sample does not flow when tilted, the jar will be held horizontally for 5 s. After that, if it

does not flow, 3 °C will be added to the corresponding temperature and the result is the pour point temperature.

Cloud Point

The cloud point of a liquid FAME mixture, which usually occurs at a higher temperature than the pour point. The cloud point is the temperature at which fuel become cloudy due to formation of crystals and solidification of saturates. Biodiesel sample will be first poured into a test jar to a level approximately half full. Then, the entire test subject will be placed in a constant temperature cooling bath. At every 1 °C, the sample will be taken out and inspected for cloud. In accordance with ASTM D2500, the oil is required to be transparent in layers 40 mm in thickness. The cloud point is the temperature at which the milky cloud crystals first appear.

4.4 Results and discussion

4.4.1 Characterization of Polybenzoxazine and Carbon Xerogel

Polybenzoxazine precursor was derived from the reaction of diamine, bisphenol-A and formaldehyde at the molar ratio of 1:1:4 via quasi-solventless approach. Dioxane was added with all reactants in order to facilitate the mixing of reactants during the synthesis.

4.4.1.1 Fourier Transform Infrared Spectroscopy (FT-IR)

The FT-IR spectrum in Figure 4.1a shows the characteristic absorption bands of partially-cured benzoxazine at 1260–1262 cm^{-1} (asymmetric stretching of C-O-C of oxazine), 1180–1187 cm^{-1} (asymmetric stretching of C-N-C), 920–950 cm^{-1} and 1491–1500 cm^{-1} (tri-substituted benzene ring). The absorption band of N-H stretching from TETA was observed around 3420–3429 cm^{-1} . Comparing with FT-IR spectrum of polybenzoxazine (Figure 4.1b), the characteristic absorption bands of fully-cured polybenzoxazine at 920–950 cm^{-1} disappeared. The structure of the fully-cured polybenzoxazine is depicted in Figure 4.2 The FT-IR results are in agreement with the study of Takeichi *et al* [11], who suggested that the characteristic absorption was transformed when ring-opening polymerization of the benzoxazine

took place. After pyrolysis, the FT-IR spectrum (Figure 4.1c) is rather flat due to the loss of all organic moieties.

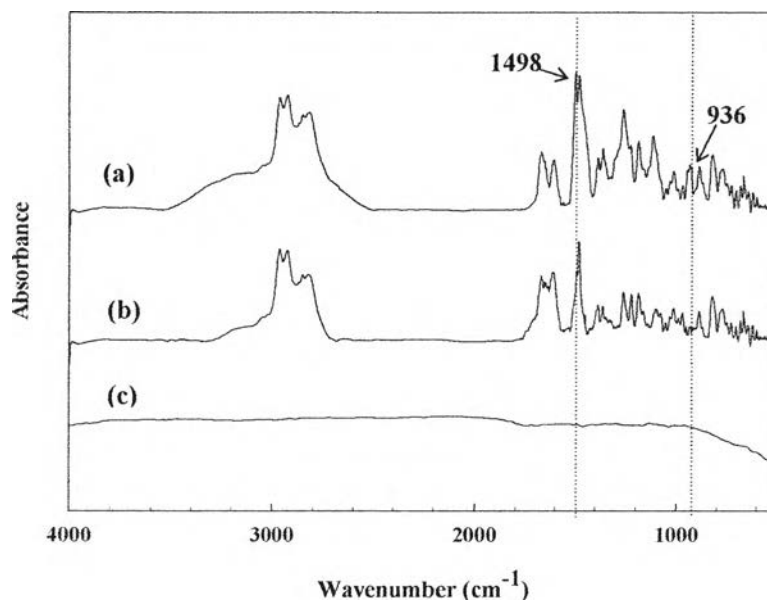


Figure 4.1 FT-IR spectra of benzoxazine precursor at 80°C (partially-cured) (a), polybenzoxazine at 200°C (fully-cured) (b), carbon xerogel at 800°C (c).

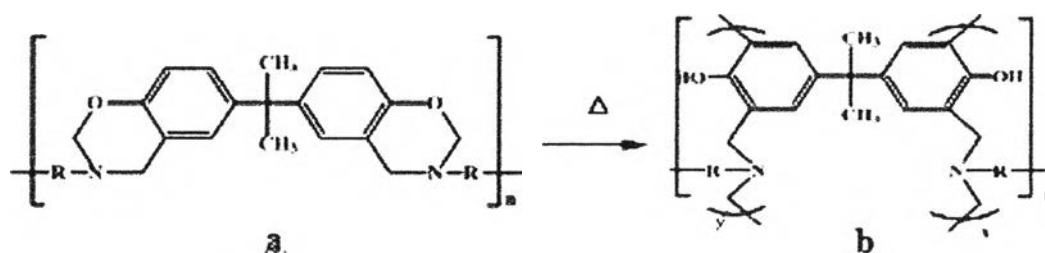


Figure 4.2 The structures of benzoxazine precursor (a), and fully-cured polybenzoxazine (b).

4.4.1.2 Surface and Pore Characteristics of Carbon Xerogel (SAA)

The specific surface area, pore volume, and pore size distribution of the supports were determined by the N_2 physisorption using a Quantachrome Autosorb-1 MP surface area analyzer. Before analyzing, the samples were heated in vacuum atmosphere at 250 °C overnight to eliminate volatile species that had ad-

sorbed on the surface. The surface and pore characteristics of carbon xerogel (CX), activated carbon (AC) and silica (SiO₂) are summarized in Table 4.1. It can be seen that the pore size of SiO₂>CX>AC respectively. In this study, The effect of pore size was considered.

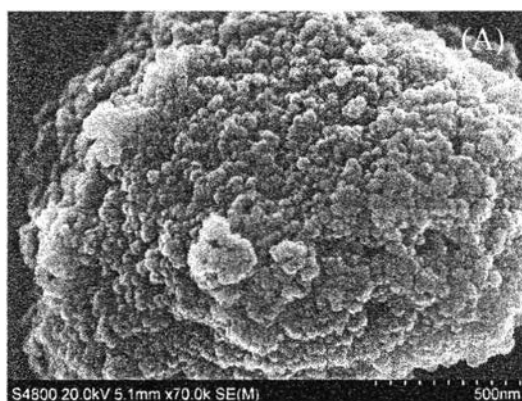
Table 4. Physical properties of AC, CX and SiO₂ used as a support in this study.

S_{BET} = Surface area, V_{total} = Total pore volume, and APD = Average pore diameter

Sample	S _{BET} (m ² /g)	V _{total} (cm ³ /g)	APD (nm)
AC	849.3	0.59	3.64
CX	513.4	3.84	29.95
SiO ₂	111	1.23	43.09

4.4.1.3 Morphology of carbon xerogel and activated carbon

The SEM micrographs reveal the pore structure of carbon xerogels prepared from polybenzoxazine via ambient drying. The structure of the carbon xerogel composed of interconnected particles in three-dimension network containing continuous mesopore (Figure 4.3B). The Figure 4.3A shows that activated carbon is a monolith carbon with rough surface consisting of micropores. On the other hand, the SEM and TEM micrographs of carbon xerogel (CX) (Figure 4.3B) show opened network structure containing large amount of various pore sizes including the mesopores were obtained from silica removal.



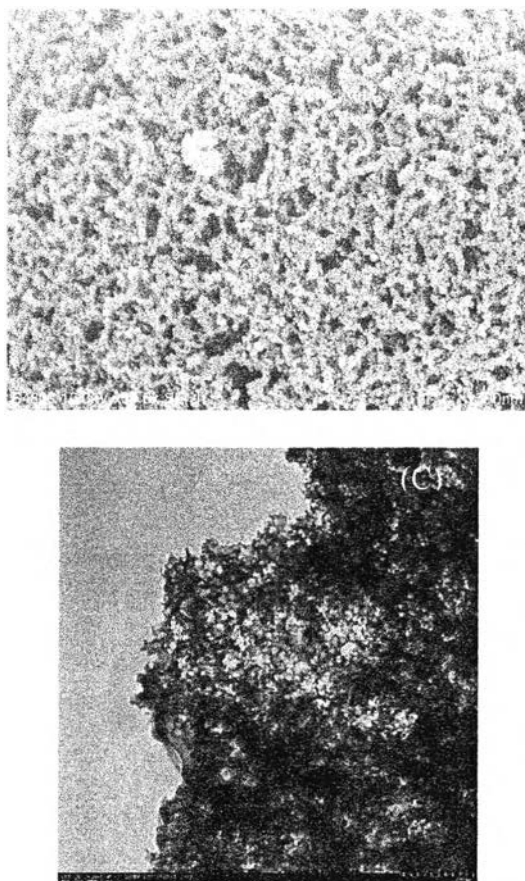


Figure 4.3 A) SEM micrographs of activated carbon, B) SEM and C) TEM micrographs of PBZ-based carbon xerogels.

4.4.2 Catalytic Activity Testing

4.4.2.1 Biodiesel upgrading by partial-hydrogenation

The effect of types of carbon support was investigated by catalytic activity testing of Pd/carbon xerogel, Pd/ activated carbon and Pd/SiO₂ in the partial hydrogenation of polyunsaturated FAMEs.

The reaction was operated at a condition of 120°C, 4 bar, 150 ml/min of hydrogen flow rate, 1000 rpm of stirring rate, and 1.0 wt.% of catalyst compared to starting oil. The percentages of C18:0, C18:1, C18:2, and other FAMEs (C12:0, C14:0, C16:0, and C22:0) after partial hydrogenation reaction for both types of carbon support are shown in Figure 4.4.

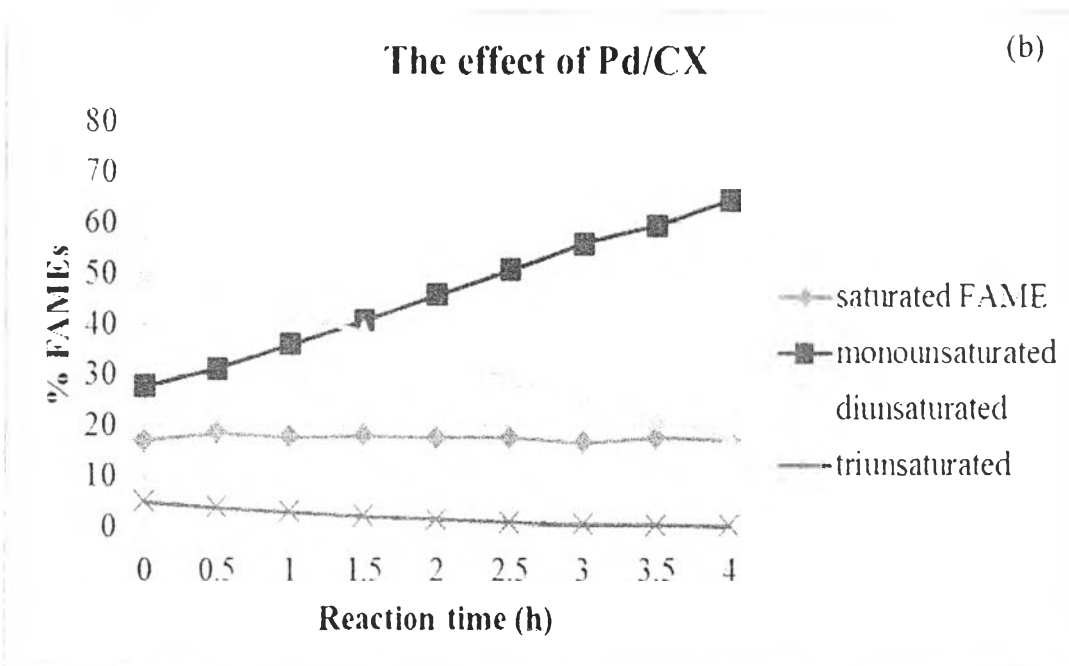
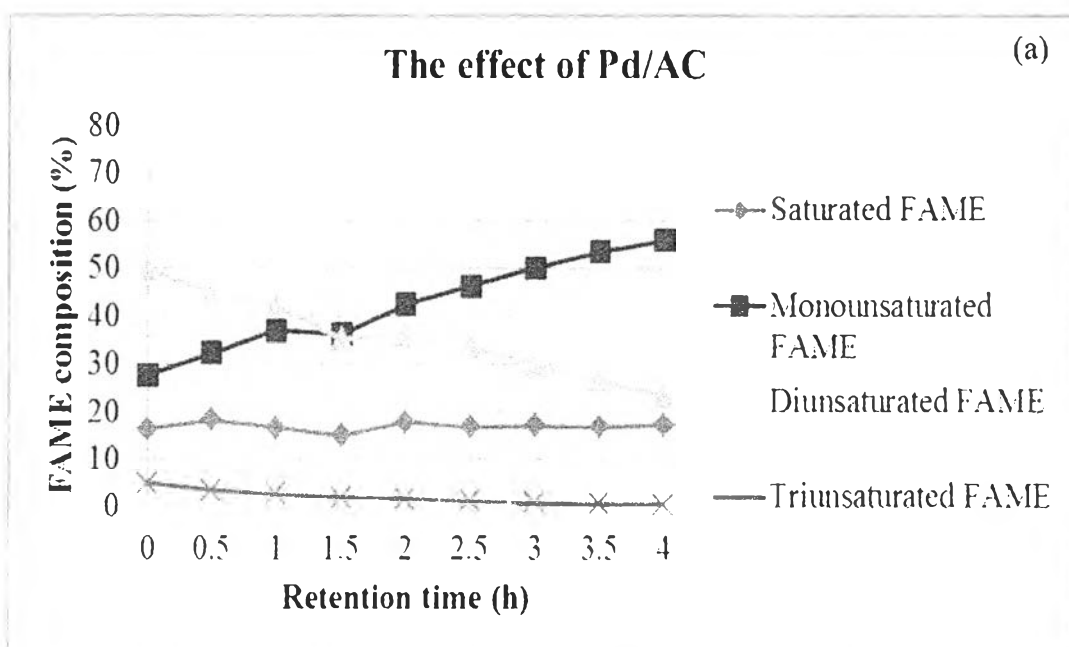
4.4.2.2 Oxidation stability

From Figure 4.4a, the Pd/activated carbon could slowly reduce C18:2; while C18:1 increased from 25% to 59% after 4 hours. C18:0 and C18:3 were steady.

When Pd/carbon xerogel was used as a support; C18:2 decreased from 50% to 20% and C18:1 increases from 25% to 65%, whereas the content of C18:0 and C18:3 were not change.

For the result of Pd/SiO₂, C18:2 was decreased from 50% to 0%; while C18:1 was increased from 30% to 75% in 4 hours. After 3 hours, C18:1 was changed to be C18:0 observe from the higher amount of graph. The increasing amount of saturated oil will effect to good oxidative stability but low cold flow property, because saturated oil can become wax when the temperature is decrease. Therefore, after 3 hour is not suitable for the reaction.

Nikolaou and co-workers (2009) suggested that the higher amounts of saturated FAMES are less prone to oxidation, but the lower cold flow property would be obtained. If we compare the relative rates of autoxidation of methyl linoleate (C18:2) which is 41 and that of methyl oleate (C18:1) which is 1; it can be deduced that the amount of C18:1 should be kept constant while decreasing the amount of C18:2 in order to improve oxidative stability without affecting the cold flow property.



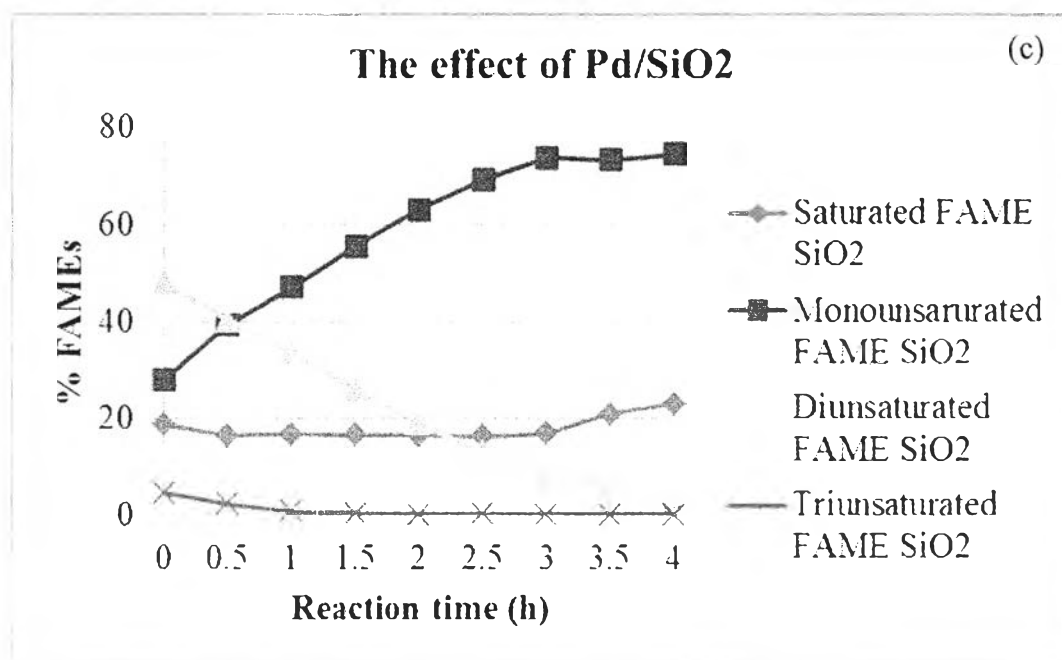
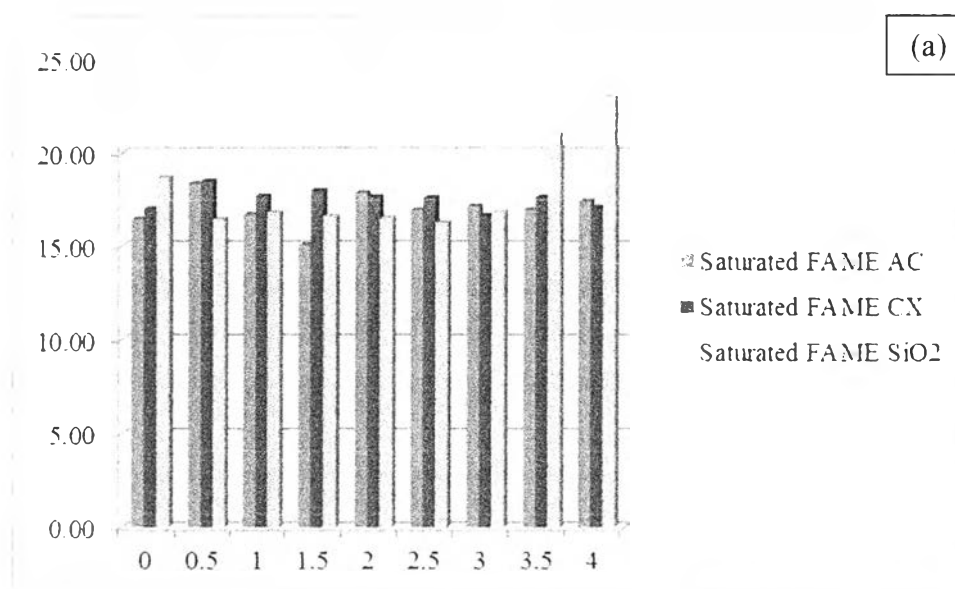


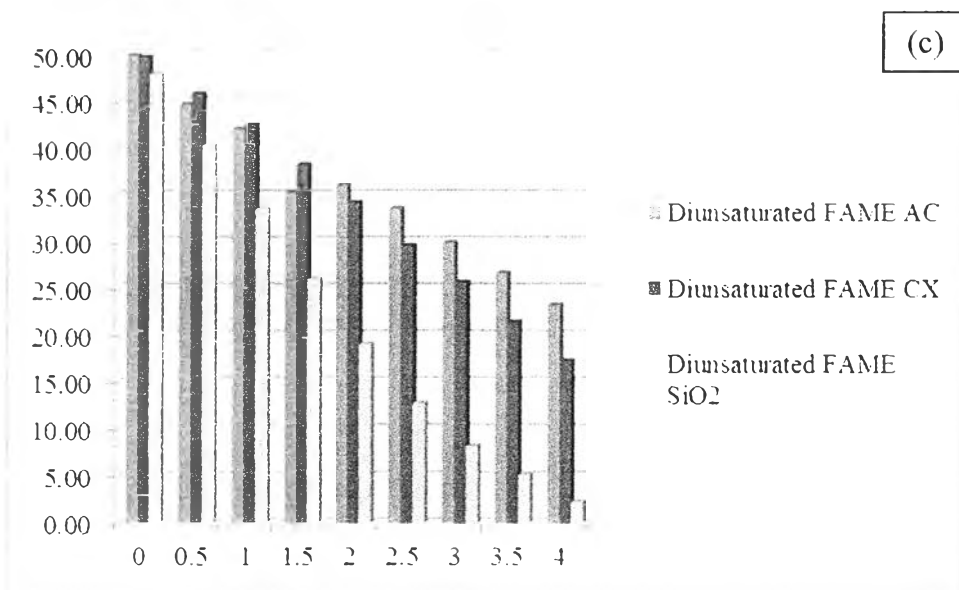
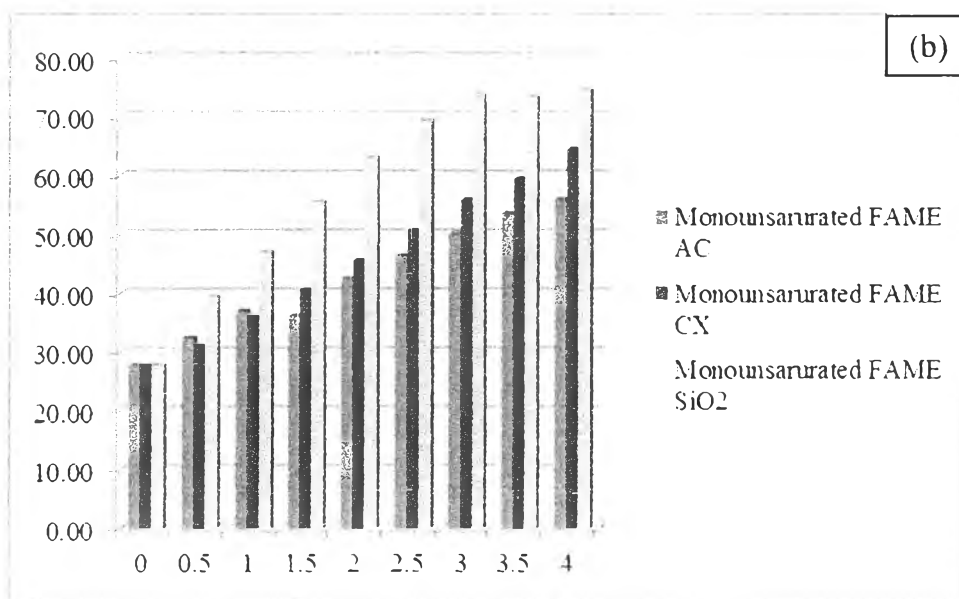
Figure 4.4 The effect of a) Pd/Activated carbon, b) Pd/Carbon xerogel, and c) Pd/SiO₂.

The bar chart showed the catalytic activities of 3 different supporting including saturated (C18:0), monounsaturated (C18:1), diunsaturated (C18:2) and triunsaturated (C18:3) under the similar condition. Silica (SiO₂) illustrated the highest activity for oxidative stability improving because it was not only make the higher monounsaturated, but also changed higher triunsaturated to diunsaturated and monounsaturated respectively. Start to discuss the amount of saturated FAMES (Figure 4.5 a), it was almost steady in 3 categories until after 3 hr. C18:1 were converse to be C18:0 then the chart of silica support was increased. The reaction time that appropriated for silica is less than 3 hr. to prevent the changing of mono- to saturated FAMES while AC and CX can be used for more long time. The second is monounsaturated (Figure 4.5 b) and diunsaturated (Figure 4.5 c), although the trend of 3 categories seem to be similar (C18:1 was amplified and C18:2 was alleviated), silica showed the highest amount of C18:1 obviously from the chart. The efficiency of CX was inferior to silica and AC was lowest. The maximum percentage conversion to monounsaturated FAMES of SiO₂, CX and AC were 75, 65 and 55% respectively, it can justified that the efficiencies of SiO₂ and CX were approximate. The last is triunsaturat-

ed (Figure 4.5 d), SiO_2/Pd converts C18:3 to the others rapidly while the conversion rate of CX/Pd and AC/Pd were slowly.

In this work, Pd particles were impregnated on three supporting materials and their catalytic activities for hydrogenation of diunsaturated to monounsaturated and saturated oil were investigated. It was found that amount of di- and triunsaturated oil were decreased while those of mono- were increased. On the other hand, the amounts of the saturated oil were almost steady. The order of the reactivity of each catalyst was as follows: $\text{Pd}/\text{AC} < \text{Pd}/\text{CX} < \text{Pd}/\text{SiO}_2$. This can be explained from a diffusion limitation of FAMES into the pores of the supports and a contact probability between FAMES on Pd active sites. In case of Pd/AC , since AC has small pore size (3.64 nm); the molecules of tri- and diunsaturated FAMES could not penetrate into these small pores (3.64 nm). suggesting that the reaction occurred at the Pd active sites located at the outer surface of the AC. Considering from the highest monounsatur. FAMES content and the lowest diunsatur. FAMES content, Pd/SiO_2 gave the best oxidative stability improvement.





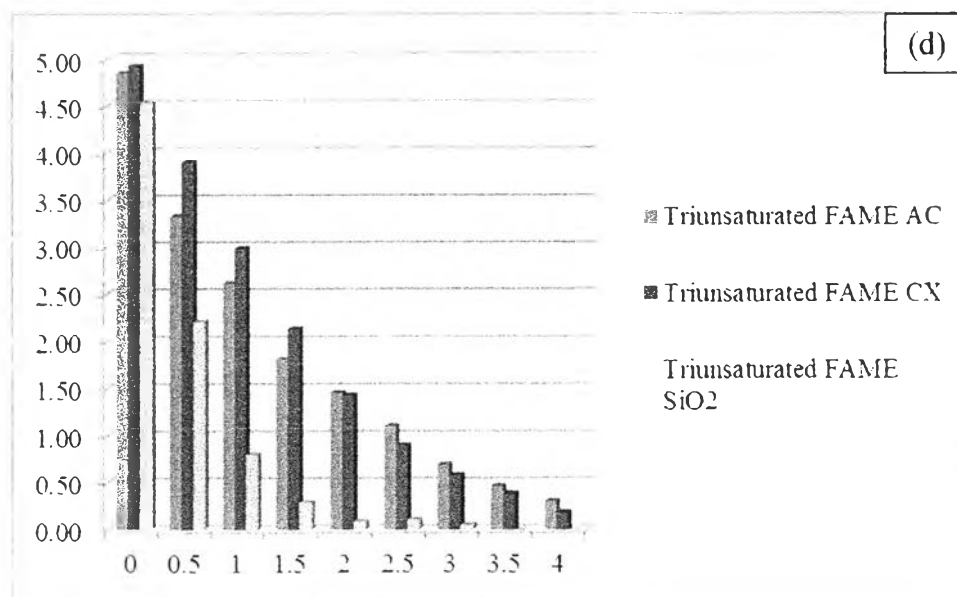


Figure 4.5 The composition of a) saturated, b) monounsaturated, c) diunsaturated and d) triunsaturated.

4.4.2.3 Cold flow property

However, the amount of cis-monounsaturated content can indicate the cold flow property which depend on the structure of the alkyl esters. The melting point decreases with the increase of double bonds. Saturated fatty acids with 10 or more carbons are solid at room temperature and their melting point increase with chain length, whereas unsaturated fatty acids are liquid. The cis- configurations in the chain can significantly reduce the melting point. Therefore, FAMEs from Pd/CX which are composed of high cis-monounsaturated and low trans-monounsaturated content have better cold flow property than those obtained from using silica template as a catalyst support.

Table 4.2 The cis-trans composition of monounsaturated FAMES content.

Reaction time	Cis-Monounsaturated FAMES		Trans-Monounsaturated FAMES	
	CX	SiO ₂	CX	SiO ₂
0 h	26.92	26.66	0.87	1.25
0.5 h	28.89	33.31	2.30	6.20
1.0 h	32.09	37.29	3.97	9.83
1.5 h	35.40	41.51	5.35	14.08
2.0 h	38.73	44.36	7.01	18.68
2.5 h	42.00	45.74	8.78	23.58
3.0 h	45.17	45.72	10.78	28.09
3.5 h	47.14	42.97	12.34	30.43
4.0 h	49.57	40.38	14.97	34.15

From Table 4.2, the results were showed in Figure 4.6-4.7. biodiesel upgrading by CX gave high content cis- composition. On the other hand, it was still gave low content trans- composition too, while cis- content of SiO₂ seem to increase at the start reaction until 3 hr. it's dropped and gave the higher trans- content with increasing reaction time. Although the large size of porous can be a good material for oxidative stability improving, it has an enough area that cis- isomer can be rearranged to trans- too. On the other hand, the size of carbon xerogel porous has not enough area for rearrangement.

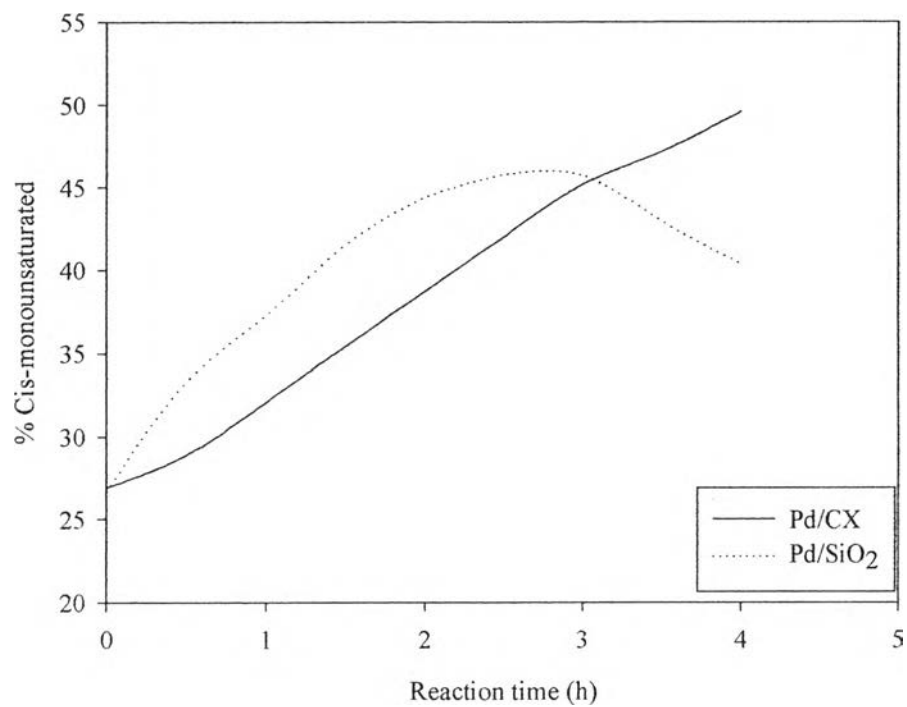


Figure 4.6 Cis- composition comparison graph between CX and SiO₂.

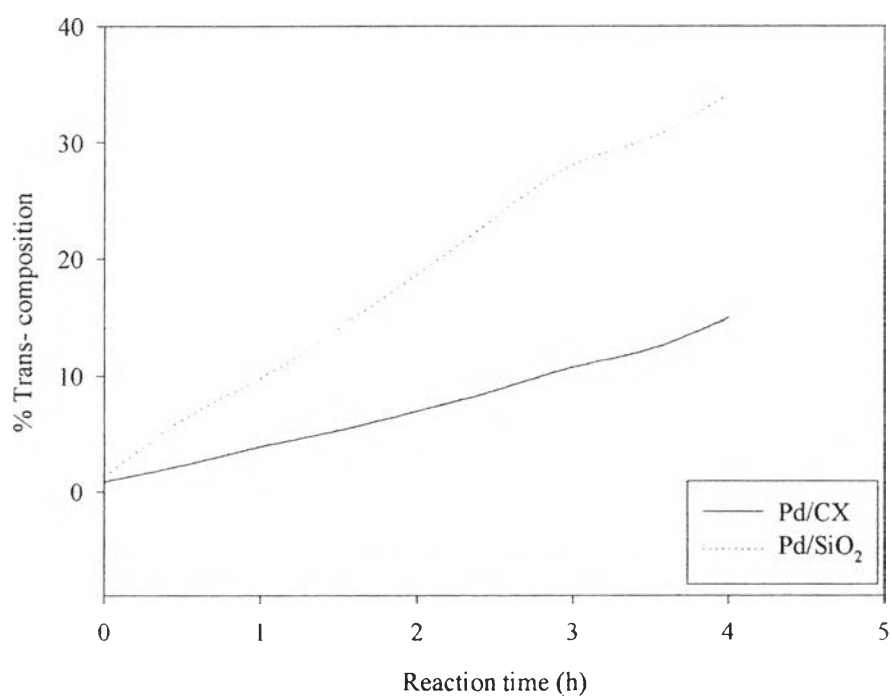


Figure 4.7 Trans- composition comparison graph between CX and SiO₂.

4.4.2.4 Properties of Biodiesel

The properties of biodiesel before and after partial hydrogenation were presented in Table 4.3. These data were analyzed by EN 14112:2003, ASTM D 2500-02, and ASTM D 6371-05 method for oxidation stability, cloud point, and filter plugging point, respectively.

After reaction finished, the hydrogenated biodiesel can be improved oxidative stability. On the contrary, cloud point and cold filter plugging point were also increased which the result from increasing saturated FAMES. Therefore, the cloud point and cold filter plugging point also depend on the content of saturated.

For the effect of pore size, activated carbon, carbon xerogel and silica are materials with surface area are 849.30, 513.40 and 111.00 nm respectively. Although surface area of silica is very high, this material is not show the best catalytic activity. Therefore, surface area is not significant on this reaction, the result of improving exhibit the oxidative stability efficiency from silica is better than carbon xerogel and activated carbon. When consider the pore size of each materials and the size of palladium 27.69 nm., palladium particle can penetrate into the pore of silica and carbon xerogel while cannot penetrate into activated carbon because the porous of activated carbon is too small. In case of activated carbon, the reaction will be occurred at the skin surface only but silica and carbon xerogel allowed reaction proceed inside the porous. Therefore, the suitable pore size is very important for the reaction.

Table 4.3 Quality analysis of biodiesel after hydrogenation.

Test Item	Result			
	Feed Biodiesel	Hydrogenated Biodiesel Pd/SiO ₂	Hydrogenated Biodiesel Pd/AC	Hydrogenated Biodiesel Pd/CX
1. Cloud Point ¹ , °C	1	6	4	3
2. Oxidation Stability at 110°C, hr	1.4	30.4	8.4	11.2
3. Cold Filter Plugging Point ² , °C	-6	0	-3	-1

¹ the temperature at which a liquid (as a petroleum oil) begins to cloud (as from the separation of wax on cooling)

² the lowest temperature, expressed in 1°C, at which a given volume of diesel type of fuel still passes through a standardized filtration device in a specified time when cooled under certain conditions. This test gives an estimate for the lowest temperature that a fuel will give trouble free flow in certain fuel systems. This is important as in cold temperate countries, a high cold filter plugging point will clog up vehicle engines more easily.

4.5 Conclusion

Partial hydrogenation of polyunsaturated FAMES of soybean biodiesel has been investigated on Pd/CX and Pd/SiO₂ catalysts. It was found that these catalysts provided good partial hydrogenation activity, resulting in an improvement of oxidative stability. Moreover, the pore size of the support had a significant effect on the activity of the catalyst and cis-monounsaturated composition. Although, silica support showed high activity on the oxidation stability improvement, Pd on the carbon xerogels support exhibited better cold flow property.

4.6 Acknowledgements

The authors would like to thank Chulalongkorn University, the Center of Excellence on Petrochemical and Materials Technology, Thailand, for their financial support. The PTT Public Company Limited for instrumental analysis support. And deeply thanks to Dr. Thanyalak Chaisuwan for suggestion. Dr. Natthida Numwong, Mr. Uthen Thubsuang, and Mr. Nattatape Jumpanoi for facilitating the work.

4.7 References

- [1] Belkacemi, K., Boulmerka, A., Arul, J., and Hamoudi, S. (2006) Hydrogenation of vegetable oils with minimum trans and saturated fatty acid formation over a new generation of Pd-catalyst. *Catalysis*, 37.

- [2] Cai, Q., Huang, Z.H., Kang, F., and Yang, J.B. (2004) Preparation of activated carbon microspheres from phenolic-resin by supercritical water activation. Carbon, 42, 775-783.
- [3] Chouhan, A.P. and Sarma, A.K. (2011) Modern heterogeneous catalysts for biodiesel production: A comprehensive review. Renewable and Sustainable Energy Reviews, 15, 4378-4399.
- [4] Drago, R., Jurczyk, K., Singh, D., and Young, V. (1995) Low-temperature deep oxidation of hydrocarbons by metal oxides supported on carbonaceous materials. Applied Catalysis B: Environmental, 6, 155-168.
- [5] Demirbas, A. (2005) Biodiesel production from vegetable oils via catalytic and non-catalytic supercritical methanol transesterification methods. Progress in Energy and Combustion Science, 31, 466-487.
- [6] Encinar, J.M., González, J.F., Sánchez, N., and Pardal, A. (2012) Soybean oil transesterification by the use of a microwave flow system. Fuel, 95, 386-393.
- [7] Fairén-Jiménez, D., Carrasco-Marín, F., and Moreno-Castilla, C. (2006) Porosity and surface area of monolithic carbon aerogels prepared using alkaline carbonates and organic acids as polymerization catalyst. Carbon, 44, 2301-2307.
- [8] Helleur, R., Popovic, N., Ikura, M., Stanciulescu, M., and Liu, D. (2001) Characterization and potential applications of pyrolytic char from ablative pyrolysis of used tires. Journal of Analytical and Applied Pyrolysis, 58-59, 813-824.
- [9] Horikawa, T., Hayashi, J., and Muroyama, K. (2004) Size control and characterization of spherical carbon aerogel particles from resorcinol-formaldehyde resin. Carbon, 42, 169-175.
- [10] Ishida, H. and Allen, D. (1996) Mechanical characterization of copolymers based on benzoxazine and epoxy. Polymer, 37, 4487-4495.
- [11] Karmee, S. and Chadha, A. (2005) Preparation of biodiesel from crude oil of *Pongamia pinnata*. Bioresource Technology, 96, 1425-1429.

- [12] Katanyoota, P., Chaisuwan, T., Wongchaisuwat, A., and Wongkasemjit, S. (2010) Novel polybenzoxazine-based carbon electrode for supercapacitors. Materials Science and Engineering B, 167, 36-42.
- [13] Knothe, G. (2008) “Designer” Biodiesel: Optimizing Fatty Composition to Improve Fuel Properties. Energy & Fuels, 22, 1358-1364.
- [14] Liu, B. and Creager, S. (2010) Carbon xerogels as Pt catalyst supports for polymer electrolyte membrane fuel-cell application. Journal of Power Sources, 195, 1812-1820.
- [15] Liu, N., Zhang, S., Fu, R., Dresselhaus, M., and Dresselhaus, G. (2006) Carbon aerogel spheres prepared via alcohol supercritical drying. Carbon, 44, 2430-2436.
- [16] Lorjai, P., Chaisuwan, T., and Wongkasemjit, S. (2009) Porous structure of polybenzoxazine-based organic aerogel prepared by sol-gel process and their carbon aerogels. Journal of Sol-Gel Science Technology, 52, 56-64.
- [17] Marchetti, J.M., Miguel, V.U., and Errazu, A.F. (2007) Possible methods for biodiesel production. Renewable and Sustainable Energy Reviews, 11, 1300-1311.
- [18] Neri, G., Musolino, M.G., Milone, C., Visco, A.M., and DiMario, A. (1995) Mechanism of 2,4-dinitrotoluene hydrogenation over Pd/C. Journal of Molecular Catalysis A Chemical, 95, 235.
- [19] Ozaki, J., Endo, N., Ohizumi, W., Igarashi, K., Nakahara, M., and Oya, A. (1997) Novel preparation method for the production of mesoporous carbon fiber from a polymer blend. Carbon, 35, 1031-1033.
- [20] Papadopoulos, C.E., Lazaridou, A., Koutsoumba, A., Kokkinos, N., Christoforidis, A., and Nikolaou, N. (2010) Optimization of cotton seed biodiesel quality (critical properties) through modification of its FAME composition by highly selective homogeneous hydrogenation. Biore-source Technology, 101, 1812-1819.
- [21] Pekala, R.W., Alviso, C.T., Kong, F.M., and Hulsey, S.S. (1992) Aerogels derived from multifunctional organic monomers. Journal of Non-crystalline Solids, 145, 90-98.

- [22] Srivastava, A. and Prasad, R. (2000) Triglycerides-based diesel fuels. Renewable and Sustainable Energy Reviews, 4, 111-133.
- [23] Tamai, H., Nobuaki, U., and Yasuda, H. (2009) Preparation of Pd supported mesoporous activated carbons and their catalytic activity. Materials Chemistry and Physics, 114, 10-13.
- [24] Thubsuang, U., Ishida, H., Wongkasemjit, S., and Chaisuwan, T. (2012) Novel template confinement derived from polybenzoxazine-based carbon xerogels for synthesis of ZSM-5 nanoparticles via microwave irradiation. Microporous and Mesoporous Material, 156, 7-15.
- [25] Xuefei, Z., Shiquan, L., Hongzhao, L., and Lijuan, G. (2009) Preparation and characterization of activated carbon foam from phenolic resin. Journal of Environmental Sciences Supplement, s121-s123.
- [26] Yang, Y., Chiang, K., and Burke, N. (2011) Porous carbon-supported catalysts for energy and environmental applications: A short review. Catalysis Today, 178, 197-205.
- [27] Yoshizawa, N., Hatori, H., Soneda, Y., Hanzawa, Y., Kaneko, K., and Dresselhaus, MS. (2003). Structure and electrochemical properties of carbon aerogels polymerized in the presence of Cu^{2+} . Journal of Non-Crystalline Solids, 330, 99-105.